Research

NMDA receptor- and ERK-dependent histone methylation changes in the lateral amygdala bidirectionally regulate fear memory formation

Swati Gupta-Agarwal, Timothy J. Jarome, Jordan Fernandez, and Farah D. Lubin[1]

Department of Neurobiology, University of Alabama at Birmingham, Birmingham, Alabama 35294, USA

It is well established that fear memory formation requires de novo gene transcription in the amygdala. We provide evidence that epigenetic mechanisms in the form of histone lysine methylation in the lateral amygdala (LA) are regulated by NMDA receptor (NMDAR) signaling and involved in gene transcription changes necessary for fear memory consolidation. Here we found increases in histone H3 lysine 9 dimethylation (H3K9me2) levels in the LA at 1 h following auditory fear conditioning, which continued to be temporally regulated up to 25 h following behavioral training. Additionally, we demonstrate that inhibiting the H3K9me2 histone lysine methyltransferase G9a (H/KMTs-G9a) in the LA impaired fear memory, while blocking the H3K9me2 histone lysine demethylase LSD1 (H/KDM-LSD1) enhanced fear memory, suggesting that H3K9me2 in the LA can bidirectionally regulate fear memory formation. Furthermore, we show that NMDAR activity differentially regulated the recruitment of H/KMT-G9a, H/KDM-LSD1, and subsequent H3K9me2 levels at a target gene promoter. This was largely regulated by GluN2B- but not GluN2A-containing NMDARs via ERK activation. Moreover, fear memory deficits associated with NMDAR or ERK blockade were successfully rescued through pharmacologically inhibiting LSD1, suggesting that enhancements of H3K9me2 levels within the LA can rescue fear memory impairments that result from hypofunctioning NMDARs or loss of ERK signaling. Together, the present study suggests that histone lysine methylation regulation in the LA via NMDAR-ERK-dependent signaling is involved in fear memory formation.

Chromatin is a dynamic structure composed of DNA wrapped around an octamer of histone proteins. N-Terminal tails of histones can undergo a variety of posttranslational modifications which leads to either activation or repression of gene transcription (Lubin et al. 2011; Jarome and Lubin 2013). Methylated lysine residues of histone tails can be mono-, di-, or trimethylated (Lachner and Jenuwein 2002; Martin and Zhang 2005) and, depending on the lysine residue methylated, a differential effect on gene transcription is observed. For example, dimethylation of histone H3 lysine 9 (H3K9me2) promotes gene silencing (Rea et al. 2000; Covington et al. 2011), whereas trimethylation of histone H3 at lysine 4 (H3K4me3) promotes gene transcription (Schneider et al. 2004; Akbarian and Huang 2009). Furthermore, these different histone methylation modifications are regulated by a unique set of histone lysine methyltransferases (H/KMT) and histone lysine demethylases (H/KDM), suggesting a coordinated regulation of histone lysine methylation modifications controls gene transcription in neurons.

In recent years numerous studies have implicated posttranslational modification of histones in the formation or "consolidation" of long-term memories in several memory-related brain regions (Levenson et al. 2004; Chwang et al. 2006; Lubin et al. 2008). For example, changes in histone lysine methylation have been shown to enhance and repress gene expression in the hippocampus and entorhinal cortex during fear memory consolidation (Gupta et al. 2010; Gupta-Agarwal et al. 2012). The amygdala is a critical site of plasticity for the formation of fear memories in the brain (LeDoux 2000). Consistent with this, inhibiting gene transcription, protein synthesis, and protein degradation in the amygdala impairs fear memory consolidation following behavioral training (Bailey et al. 1999; Parsons et al. 2006; Jarome et al. 2011) leading to the theory that a coordinated regulation of changes in gene transcription in the amygdala is necessary for the formation of fear memories (Johansen et al. 2011; Jarome and Helmstetter 2013). However, although some studies have suggested a role for posttranslational modification of histone mediated chromatin remodeling in the consolidation of fear memories in the amygdala (Koshibu et al. 2009; Monsey et al. 2011; Mahan et al. 2012), it is unknown if histone lysine methylation is required for lateral amygdala (LA)-dependent fear memory consolidation. Furthermore, very little is known about how histone lysine methylation is regulated during fear memory consolidation.

In the present study, we found that fear conditioning increased H3K9me2 levels in the LA and that inhibiting H/KMTs-G9a or H/KDM-LSD1 activity for H3K9me2 in the LA impaired or enhanced fear memory, respectively. Additionally, these changes in H3K9me2 were dependent on GluN2B containing NMDA receptors (NMDARs) and ERK signaling. Further inhibiting H/KDM-LSD1 activity for H3K9me2 rescued memory deficits induced by pharmacological blockade of NMDAR or ERK signaling. Together, these findings highlight an important role for NMDA-ERK signaling in coordinated changes in histone lysine methylation in the LA that are necessary for fear memory consolidation.

[1]**Corresponding author**
E-mail flubin@uab.edu
Article is online at http://www.learnmem.org/cgi/doi/10.1101/lm.035105.114.

Results

Histone H3 lysine methylation in the LA

To investigate whether histone lysine methylation is altered in the LA during memory consolidation, we used an auditory fear conditioning paradigm since this type of cued fear conditioning relies primarily on the amygdala for its acquisition and long-term memory storage (Phillips and LeDoux 1992). In our learning paradigm, animals were placed in a novel context and presented with several pairings of an auditory cue that co-terminated with a brief footshock (Trained). A separate group of animals was exposed to the auditory cue presentations in the training context but did not receive the shock presentations (Tone). This group served as an associative memory control since animals do not learn to associate the auditory cue with the footshock (Jarome et al. 2011). LA tissue was then collected 1 h after fear conditioning and histone lysine methylation levels were analyzed using western blotting (Fig. 1A). We found significant increases in H3K9me2 levels in the LA 1 h after fear conditioning in trained animals ($t_{(7)} = 2.615$, $P < 0.05$) but not in tone-only exposed animals compared to naïve homecaged controls ($t_{(7)} = 1.327$, $P = 0.775$). Interestingly, we did not find changes in H3K4me3 levels, a transcriptionally active mark, in the LA 1 h after fear conditioning in trained animals ($t_{(6)} = 0.7619$, $P = 0.6708$), but H3K4me3 levels increased with tone-only exposed animals compared to naïve homecaged controls ($t_{(7)} =$

2.429, $P < 0.05$). These results suggest that the transcriptional repressive mark H3K9me2, but not the transcriptional activity mark H3K4me3, in the LA is specific to associative fear learning.

Because *G9a* gene expression is regulated by H3K9me2 (Gupta-Agarwal et al. 2012), we next assessed the gene expression profile of *G9a* in the LA during fear memory formation. Gene expression studies revealed that *G9a* mRNA levels were significantly decreased in the LA 1 h after fear conditioning in trained animals ($t_{(7)} = 6.229$, $P < 0.001$) (Fig. 1B) but were significantly increased in the LA of tone-only exposed animals compared to naïve controls ($t_{(7)} = 2.655$, $P < 0.05$). These data suggest that decreases in *G9a* gene expression in the LA following fear conditioning correlate with increased H3K9me2, a repressive mark of transcription. Furthermore, these results indicate that *G9a* gene expression serves as an ideal candidate for regulation by H3K9me2 methylation in the LA during fear memory consolidation.

Although we observed increases in H3K9me2 levels and decreases in *G9a* mRNA expression in the LA of animals exposed to pairings of the tone and shock but not the tone alone, it is possible that exposure to the brief footshock alone is sufficient to drive these changes. To rule out this possibility, we exposed a separate cohort of animals to an immediate footshock presentation and compared them with animals that received pairings of the tone and footshock. We found significant increases in H3K9me2 levels in the LA of trained animals ($t_{(9)} = 2.363$, $P < 0.05$) but not of the footshock exposed alone animals ($t_{(8)} = 0.994$, $P = 0.349$) relative to naïve controls (Fig. 1C). Additionally, H3K4me3 levels in the LA of trained ($t_{(9)} = 0.084$, $P = 0.934$) or footshock exposed alone animals ($t_{(8)} = 0.792$, $P = 0.451$) remained unchanged relative to naïve controls. However, consistent with the observed increases in H3K9me2 levels in the LA following fear conditioning, we found a significant reduction in *G9a* expression in the trained group ($t_{(7)} = 3.370$, $P < 0.05$) but not when animals were exposed to the footshock alone ($t_{(7)} = 0.914$, $P = 0.390$) compared to the naïve control group (Fig. 1D). Together, these results confirm that increases in H3K9me2 levels and decreases in *G9a* mRNA expression in the LA were specific to the association of the auditory cue with the shock during training.
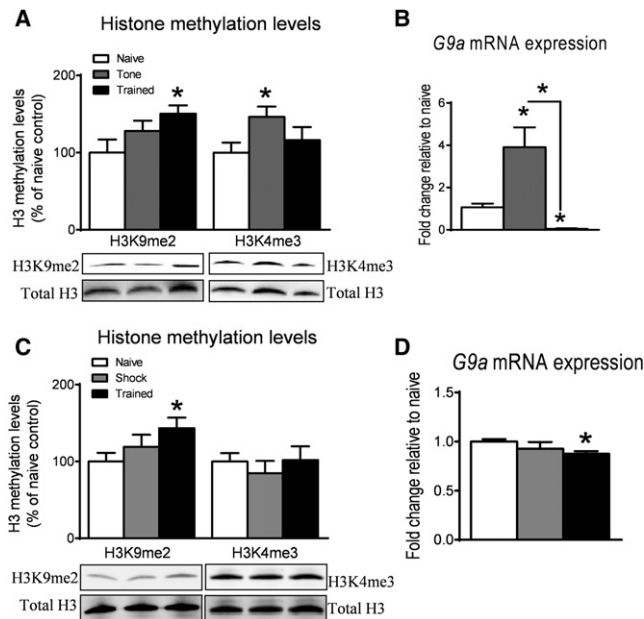
Figure 1. Alterations in histone methylation and *G9a* expression in the LA during long-term memory formation. (*A*) Animals were trained to auditory fear conditioning (trained) or exposed to the auditory cue without footshock (tone). Western blotting analysis showed a significant increase in H3K9me2 levels in the LA of trained animals compared to naïve controls 1 h following fear conditioning and significant increases in H3K4me3 levels in the LA of tone animals compared to naïve controls 1 h following fear conditioning ($n = 4$–5). (*B*) Real-time qPCR revealed significant increases in *G9a* mRNA of tone animals compared to naïve controls; however, *G9a* mRNA was significantly decreased in the LA of trained animals compared to naïve controls and tone animals ($n = 4$–5). (*C*) Western blotting analysis showed a significant increase in H3K9me2 levels in the LA of trained animals compared to naïve controls 1 h following fear conditioning with no changes in H3K4me3 levels in the LA of immediate shock animals compared to naïve controls 1 h following fear conditioning ($n = 5$–6). (*D*) Real-time qPCR revealed significant decreases in *G9a* mRNA in the LA of trained animals compared to naïve controls with no changes in the immediate shock group ($n = 5$–6). (*) $P < 0.05$.

The lasting effect of auditory fear conditioning on histone H3 lysine methylation levels in the LA

Since histone lysine methylation marks can be both transiently and persistently regulated in neurons, we sought to determine whether or not histone methylation alterations were persistently regulated in the LA at 24 h following auditory fear conditioning. For these experiments, animals were trained to auditory fear conditioning or exposed to the tone-alone, and histone methylation levels in the LA were assessed 24 h later (Fig. 2A). We found a significant decrease in H3K9me2 levels in the LA of trained animals compared to naïve homecaged controls ($t_{(4)} = 3.276$, $P < 0.05$), with no changes observed in the LA of tone-only exposed animals ($t_{(5)} = 0.929$, $P = 0.063$). However, H3K4me3 levels were not significantly altered in the LA of trained ($t_{(5)} = 0.176$, $P = 0.728$) or tone-only exposed animals ($t_{(5)} = 0.837$, $P = 0.393$) compared to naïve homecaged controls. These results suggest that, unlike the H3K4me3 transcription activation mark, the H3K9me2 transcription repressive mark is dynamic and continues to be regulated in the LA at 24 h following fear conditioning training. Because *G9a* expression is regulated by H3K9me2 levels, we investigated *G9a* gene mRNA levels in the same cohort of animals (Fig. 2B) and found no significant alterations in *G9a* mRNA levels in the LA of tone-only exposed ($t_{(6)} = 0.946$, $P = 0.178$) and trained animals ($t_{(6)} = 1.553$, $P = 0.147$) compared to naïve homecaged controls, though *G9a* expression remained marginally reduced relative to naïve controls. Collectively, these results suggest persistent
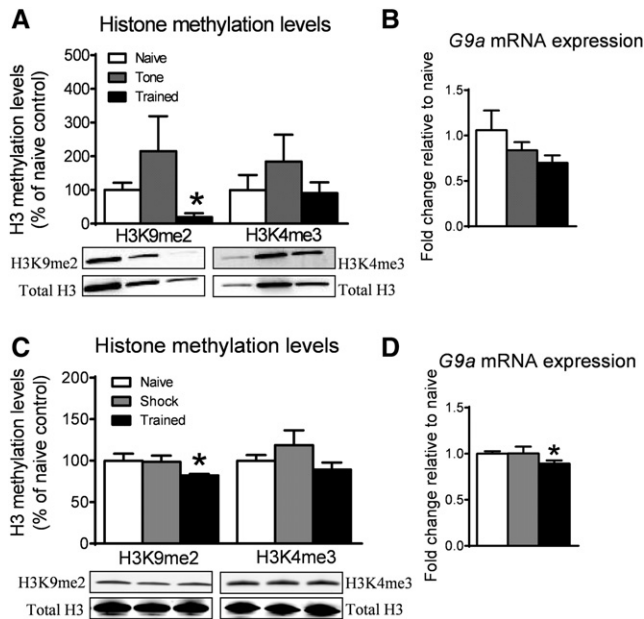
Figure 2. Histone methylation continues to be temporally regulated in the LA after the completion of the memory consolidation process. (*A*) There were significant decreases in H3K9me2 levels in the LA of trained animals compared to naïve control 24 h after fear conditioning. No change was observed in H3K4me3 levels across the three groups at 24 h ($n = 4–5$). (*B*) Real-time qPCR analysis of *G9a* mRNA revealed no significant change across the three groups at 24 h after fear conditioning. (*C*) Western blotting revealed a significant reduction in H3K9me2 levels in trained animals relative to naïve controls, without any changes in H3K4me3 levels. (*D*) Real-time qPCR analysis of *G9a* mRNA revealed a significant reduction in the trained group relative to the naïve group ($n = 4–6$ per group). (*) $P < 0.05$.

regulation of the H3K9me2 methylation long after the consolidation phase of fear memory.

To confirm that H3K9me2 levels and *G9a* expression in the LA at 24 h after behavioral training were specific to associative fear learning, we exposed a separate group of animals to the immediate footshock alone and assessed H3K9me2 levels in the LA compared with the effect on histone methylation levels in the LA of trained animals. Consistent with our previous results, we found a significant decrease in H3K9me2 levels in the LA of trained ($t_{(8)} = 2.533$, $P < 0.05$), but not with footshock exposure alone ($t_{(7)} = 0.120$, $P = 0.907$), compared to naïve homecaged controls (Fig. 2C), suggesting persistent regulation of this epigenetic mark, well beyond the consolidation phase. Additionally, we observed no changes in H3K4me3 levels in the LA at 24 h in the footshock alone ($t_{(7)} = 0.896$, $P = 0.399$) or trained ($t_{(8)} = 0.907$, $P = 0.390$) groups relative to naïve homecaged controls. Interestingly, we did find a significant reduction in *G9a* mRNA levels in the LA of trained ($t_{(7)} = 2.367$, $P < 0.05$) but not footshock alone ($t_{(7)} = 0.021$, $P = 0.983$) groups relative to naïve homecaged animals (Fig. 2D). Together, these results suggest that both H3K9me2 levels and *G9a* mRNA expression continue to be regulated long after the consolidation phase.

The effect of inhibiting H/KMT-G9a or H/KDM-LSD1 activity in the lateral amygdala during memory consolidation

The sum levels of H3K9me2 in eukaryotic cells reflect the opposing activities of the H/KMT-G9a, which promotes H3K9me2

(Tachibana et al. 2001, 2002, 2005, 2008), and H/KDM-LSD1, which removes the H3K9me2 modification (Metzger et al. 2005). Therefore, we addressed whether the H3K9me2 mark in the LA was critical for fear memory formation by pharmacologically inhibiting H/KMT-G9a activity, resulting in decreased H3K9me2 levels, or inhibiting H/KDM-LSD1 activity, resulting in enhanced H3K9me2. For these experiments, we infused the potent and selective H/KMT-G9a inhibitor UNC0224 (Liu et al. 2009) or saline-vehicle bilaterally into the LA 1 h prior to fear conditioning and tested retention to the auditory cue 24 h later (Fig. 3A). We found no significant differences in freezing behavior during the training session ($t_{(17)} = 0.191$, $P = 0.834$). These results suggest that UNC0224 treatment did not affect memory acquisition and that inhibiting H/KMT-G9a activity with UNC0224 impaired memory consolidation for the auditory cue, as freezing behavior significantly decreased on test-day (24 h later) compared to vehicle controls ($t_{(14)} = 2.758$, $P < 0.05$). Alternatively, while inhibiting H/KDM-LSD1 in the LA with *trans*-2-phenylcyclopropylamine (t-PCP) (Binda et al. 2010; Benelkebir et al. 2011) prior to fear conditioning did not alter behavioral performance during the training session ($t_{(15)} = 0.512$, $P = 0.553$), H/KDM-LSD1 inhibition enhanced fear memory for the auditory cue on Test-day (24 h later) when compared to vehicle controls ($t_{(28)} = 2.194$, $P < 0.05$) (Fig. 3B). Collectively, these findings indicate that dynamic regulation of the H3K9me2 mark by H/KMT-G9a or H/KDM-LSD1 in the LA following fear conditioning can act as a bidirectional regulator of fear memory formation.

We next determined the effect of H/KDM-LSD1 inhibition by t-PCP on dynamic recruitment of LSD1, H/KMT-G9a, and H3K9me2 at the *G9a* promoter in response to NMDAR activation. Using chromatin immunoprecipitation (ChIP), studies were
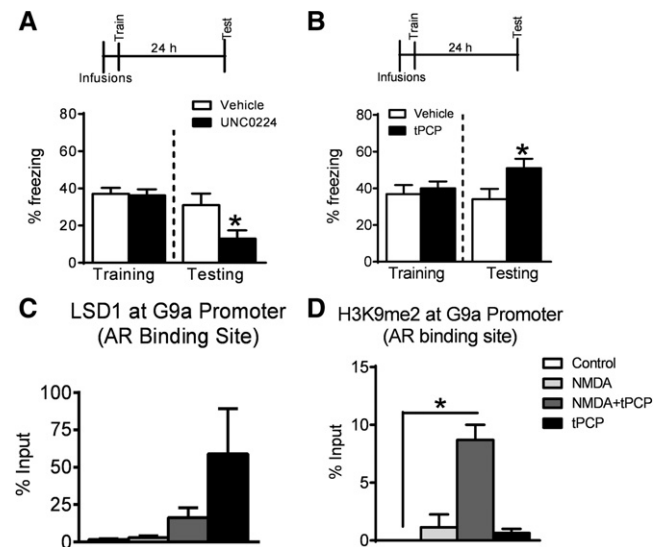

Figure 3. Inhibition of HMT-G9a interferes with memory formation in the LA whereas inhibition of HDM-LSD1 enhances memory formation. Animals were infused with the G9a inhibitor UNC0224 or the LSD1 inhibitor t-PCP into the LA 1 h prior to fear conditioning. (*A*) Intra-LA UNC0224 infusions did not alter performance during the training session but UNC0224 infused animals froze significantly less than vehicle controls on the test ($n = 7–9$). (*B*) Intra-LA t-PCP infusions did not alter performance during the training session but t-PCP infused animals froze significantly more than vehicle controls on the test ($n = 14–17$). (*C*) ChIP analysis on LA brain slices revealed no significant changes in HDM-LSD1 binding at G9a PW1 following 1-h application of NMDA or NMDA+t-PCP or t-PCP. (*D*) ChIP analysis revealed significant increases in H3K9me2 occupancy binding at G9a PW1 in NMDA+t-PCP group compared to the vehicle-control ($n = 3–4$). (*) $P < 0.05$.

undertaken in LA slices ex vivo at 1 h following NMDAR activation, either in the absence (NMDA) or presence of t-PCP (NMDA+t-PCP). We found a main effect for the drug on H/KDM-LSD1 ($H_{(4)}$ = 8.013, $P < 0.05$) and H3K9me2 levels ($H_{(4)}$ = 9.359, $P < 0.01$) at the *G9a* promoter (Fig. 3C,D); however, Dunn's post hoc tests did not reveal significant differences in H/KDM-LSD1 binding levels at the *G9a* promoter in the NMDA, t-PCP, or NMDA+t-PCP treated groups compared to the control group (Fig. 3C). H/KDM-LSD1 enzymatic activity, but not its histone binding site, is blocked by t-PCP, suggesting that these results are in agreement with t-PCP mediated inhibition of H/KDM-LSD1 activity on H3K9me2. Consistent with this, we found significant enhancements in H3K9me2 levels at the *G9a* gene promoter in the NMDA+t-PCP group compared to the control group (Fig. 3D), supporting increased H3K9me2 binding at the *G9a* promoter following NMDA stimulation in the absence of H/KDM-LSD1. Collectively, these results confirm inhibition of H/KDM-LSD1 activity but not binding by t-PCP at the *G9a* promoter.

H/KMT-G9a, H/KDM-LSDl, and H3K9me2 regulation in the lateral amygdala requires NMDAR activity

It has been well established that NDMAR activity in the LA is critical for memory formation (Malkani and Rosen 2001; Bauer et al. 2002; Sah et al. 2008) and impaired NMDAR function has been observed in several neurological disorders that are associated with memory deficits (Son et al. 2006; Marek et al. 2010; Szakacs et al. 2012). Therefore, we examined whether H/KDM-LSD1 and H/KMT-G9a may be downstream targets of NMDAR activation in the LA during memory consolidation by testing if NMDA receptor activity controls changes in the binding of H/KDM-LSD1 and H/KMT-G9a of the *G9a* promoter in the LA ex vivo. For these experiments, LA brain slices were subjected to ChIP studies following incubation for 1 h with vehicle-control alone (Control), NMDA (NMDA), or NMDA plus the NMDA antagonist MK801 (NMDA+MK801). We found a main effect for H/KDM-LSD1 ($H_{(3)}$ = 6.167, $P < 0.05$) (Fig. 4B) binding levels at the *G9a* promoter walk (PW) site 1 and a trend for a main effect for H/KMT-G9a ($H_{(3)}$ = 5.422, $P = 0.071$) (Fig. 4A) binding levels, suggesting altered binding of the *G9a* promoter following NMDA stimulation and/or blockade. We next expanded the *G9a* promoter region profiled to include 5000 bp upstream of the transcriptional start site (TSS). Importantly, the sheared chromatin was restricted to the 500 bp range to limit primer overlap. We found a significant main effect for H/KMT-G9a binding levels at the *G9a* PW site 2 ($H_{(3)}$ = 6.167, $P < 0.05$), suggesting altered binding following NMDA stimulation, and a trend for a main effect at *G9a* PW site 6 ($H_{(3)}$ = 5.440, $P = 0.058$). However, we did not observe main effects for HKMT-G9a binding levels at the *G9a* PW sites 3 ($H_{(3)}$ = 2.575, $P = 0.293$), 4 ($H_{(3)}$ = 2.220, $P = 0.353$), 5 ($H_{(3)}$ = 2.808, $P = 0.277$), and 7 ($H_{(3)}$ = 4.212, $P = 0.129$). These studies suggest, for the first time, differential H/KMT-G9a binding across the *G9a* promoter in the LA. Analysis of H/KDM-LSD1 across the *G9a* promoter revealed main effects for binding at *G9a* PW sites 4 ($H_{(3)}$ = 7.053, $P < 0.01$), 5 ($H_{(3)}$ = 7.636, $P < 0.01$), 6 ($H_{(3)}$ = 5.932, $P < 0.05$), and 7 ($H_{(3)}$ = 5.357, $P < 0.05$), with a significant decrease only at *G9a* PW site 5 in the NMDA group in comparison to controls. Together, these findings suggest that not only does NMDA differentially recruit H/KMT-G9a and H/KDM-LSD1 at the *G9a* gene promoter but the two antagonistic enzymes are not mutually exclusive depending on the specific binding site assessed across a given gene promoter such as *G9a*.

Because the ultimate read-out of both H/KMT-G9a and H/KDM-LSD1 activity is H3K9me2, we next investigated the H3K9me2 profile across the *G9a* promoter in the same sample sets described above (Fig. 4C). We found significant effects in
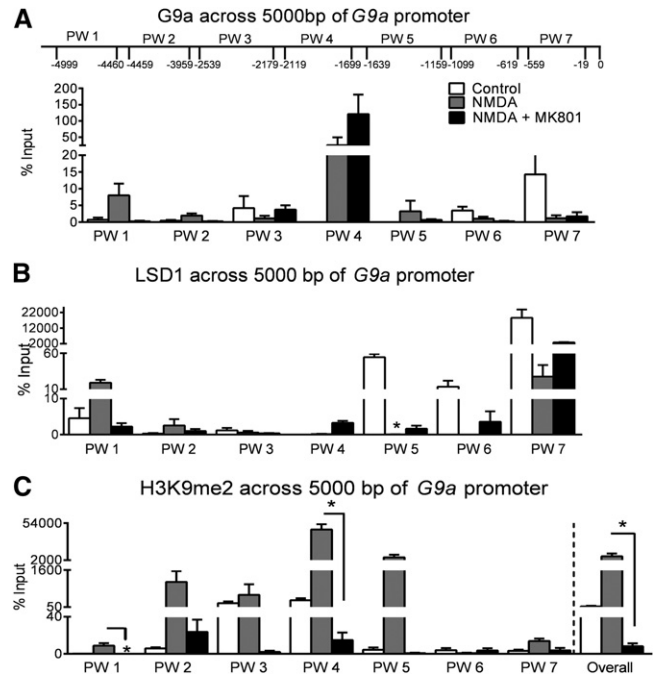
Figure 4. NMDA receptor activity differentially regulates H3K9me2, HMT-G9a, and HDM-LSD1 at the *G9a* promoter in the LA. Ex vivo analysis of NMDA receptor mediated binding of H3K9me2, HMT-G9a, and HDM-LSD1 at the *G9a* promoter in the LA. Slices were incubated for 1 h with NMDA, NMDA+MK801, or control prior to ChIP analysis. (*A*) Differential binding of HMT-G9a across 5000 bp of *G9a* promoter in the LA ($n = 3–5$). (*B*) Differential binding of HDM-LSD1 across 5000 bp of *G9a* promoter in the LA. NMDA stimulation decreased binding at PW site 5 relative to controls ($n = 3–5$). (*C*) Differential binding of H3K9me2 across 5000 bp of *G9a* promoter in the LA. NMDA enhanced binding at PW sites 1 and 4, which was reversed by MK801 ($n = 3–5$). Overall H3K9me2 occupancy at the G9a promoter revealed a significant increase in the presence of NMDA compared to the NMDA+MK801 group ($n = 23–27$). (*) $P < 0.05$.

H3K9me2 binding levels at *G9a* PW sites 1 ($H_{(3)}$ = 8.326, $P < 0.01$), 2 ($H_{(3)}$ = 5.762, $P < 0.05$), and 4 ($H_{(3)}$ = 8.018, $P < 0.01$). Interestingly, the enhancements in H3K9me2 binding levels at *G9a* PW sites 1 and 4 assessed in the NMDA group were successfully blocked by MK801. Furthermore, the overall profile of H3K9me2 binding across the *G9a* promoter revealed an enhancement in the presence of NMDA that was significantly reduced in the NMDA+MK801 group ($H_{(3)}$ = 13.47, $P < 0.01$), supporting that increases in H3K9me2 binding across the *G9a* promoter are dependent upon NMDA receptor activity.

The findings described above suggest that there is an overall increase in the suppressive chromatin microenvironment of the *G9a* promoter in response to NMDAR signaling. In support of this, we found significant enhancement in H/KMT-G9a and H3K9me2 binding levels at the *G9a* promoter sites that correlated with decreased H/KMT-G9a protein expression observed upon NMDAR stimulation ($t_{(4)}$ = 3.184, $P < 0.05$) (Fig. 5A), which is prevented by stimulating NMDARs in the presence of MK801 ($t_{(4)}$ = 3.447, $P < 0.05$). Furthermore, bioinformatics at the *G9a* promoter revealed important regulatory putative binding sites for several transcription factors such as CREB and NF-κB. The presence of these various transcription factor consensus sites along the *G9a* promoter may contribute to the differential binding of H/KMT-G9a, H/KDM-LSD1, and H3K9me2 observed at these sites. Additionally, an important observation was the presence of a putative androgen receptor (AR) binding contained within
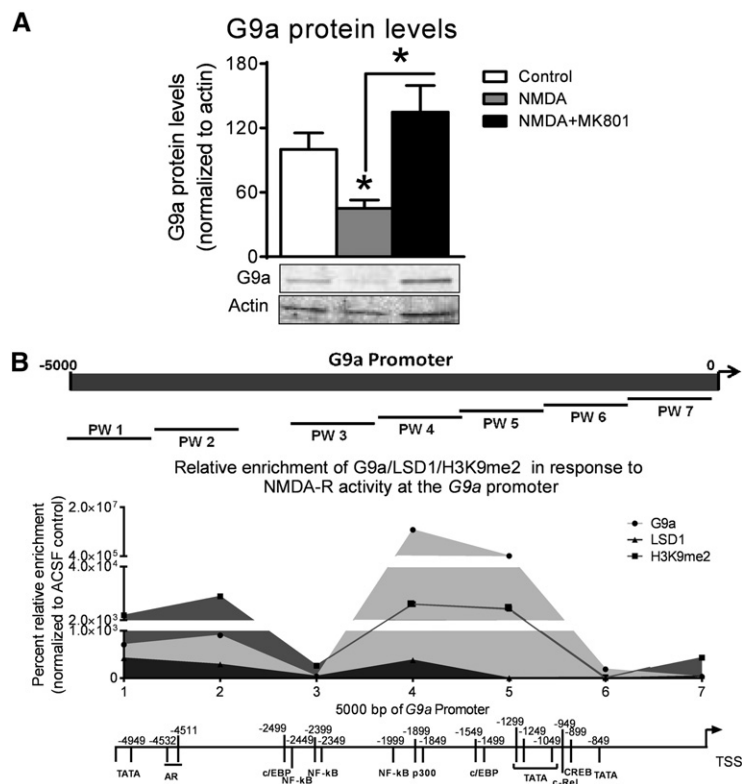
G9a PW site 1 (Fig. 5B), as it has been established that LSD1 in complex with the AR functions to specifically de-methylate H3K9me2 (Metzger et al. 2005; Wang et al. 2007). Collectively, these results suggest that NMDAR activity differentially regulates the recruitment of H/KMT-G9a, H/KDM-LSD1, and H3K9me2 to gene promoters such as *G9a* in the LA.

GluN2B and GluN2A NMDAR containing subunits differentially regulate H3K9me2

NMDAR properties are dependent on its subunit composition (Furukawa et al. 2005; Flores-Soto et al. 2012). Generally, NMDARs are found in a heteromeric state composed of two copies each of the glycine binding GluN1 subunits, glutamate binding-GluN2 subunit and/or GluN3 subunits (Furukawa et al. 2005; Flores-Soto et al. 2012). In the LA, NMDARs are largely composed of either the GluN2A or GluN2B subunit in addition to the GluN1 subunit (Schito et al. 1997) and it has been shown that the GluN2B subunit is critical for fear learning, whereas the GluN2A subunit has stronger implications in fear expression (Rodrigues et al. 2001). Indeed, overexpression of the GluN2B subunit in genetically modified mice revealed enhanced fear-conditioned performance relative to wild-type controls (Tang et al. 1999). Therefore, we sought to determine which NMDAR subunit, GluN2B or GluN2A, regulates H3K9me2 levels at the *G9a* promoter within the LA.

Figure 5. NMDA receptor activity down-regulates G9a protein levels in the LA. (*A*) LA slices were incubated for 1 h with NMDA, NMDA+MK801, or control. Western blot analysis revealed significant decreases in G9a protein in NMDA group compared to controls and NMDA+MK801 group (*n* = 3). (*B*) Primer design across 5000 bp of *G9a* promoter, 0 marks the transcription start site. Graphical presentation of the relative enrichment of H/KMT-G9a, H/KDM-LSD1, and H3K9me2 across the *G9a* promoter in the presence of NMDAR agonist. Bioinformatic analysis revealed several transcription factor binding sites across 5000 bp of *G9a* promoter. (*) *P* < 0.05.

LA brain slices were subject to ChIP studies following incubation for 1 h with vehicle controls alone (controls), NMDA alone (NMDA), or NMDA plus the GluN2A specific antagonist NVP AAM 077 (NMDA+NVP AAM 077) or with the GluN2A specific antagonist alone (NVP AAM 077) (Mallon et al. 2005). We restricted the *G9a* promoter analysis to PW sites that showed dense transcriptional factor binding and/or where H3K9me2 binding levels were significantly altered in response to NMDAR activity (Fig. 4). We found main effects for H3K9me2 binding levels at *G9a* PW sites 2 ($H_{(4)} = 10.46$, $P = 0.001$) and 4 ($H_{(4)} = 8.173$, $P < 0.05$), with a trend for an effect at site 1 ($H_{(4)} = 7.427$, $P = 0.059$). Interestingly, blockade of GluN2A with NVP AAM 077 increased H3K9me2 levels at the *G9a* PW site 2. This result suggests that the GluN2A subunit of the NMDAR does not regulate the H3K9me2 levels at the *G9a* promoter within the LA upon NMDAR activation. Additionally, the overall profile of H3K9m2 binding across the *G9a* promoter did not reveal a significant effect of manipulating NMDAR or GluN2A activity ($H_{(4)} = 7.210$, $P = 0.065$), further supporting that the GluN2A subunit of the NMDAR does not regulate H3K9me2 levels at the G9a promoter following NMDAR activation.

To determine whether the GluN2B subunit of the NMDAR contributed to H3K9me2 regulation in the LA, brain slices were subject to ChIP studies following incubation for 1 h with vehicle control alone (controls), NMDA alone (NMDA), or NMDA plus the GluN2B specific antagonist Ro25-6981 (NMDA+Ro25-6981) (Fischer et al. 1997) or Ro25-6981 alone (Ro25-6981) (Fig. 6B).

Analysis of H3K9me2 binding levels across the *G9a* promoter was largely in agreement with our MK801 studies (Fig. 4). Specifically, we found main effects for H3K9me2 binding levels at *G9a* PW sites 4 ($H_{(4)} = 8.197$, $P < 0.01$) and 5 ($H_{(4)} = 8.808$, $P < 0.01$) and the alterations at PW site 4 were largely similar to those observed in our MK801 studies. Supporting this, the overall profile of H3K9me2 binding across the *G9a* promoter revealed a main effect ($H_{(4)} = 11.06$, $P < 0.05$), revealing a significant reduction in H3K9me2 binding at the G9a promoter following NMDA stimulation in the presence of Ro25-6981. Together, these results suggest that the GluN2B NMDAR subunit plays an important role in regulating both basal and activity NMDAR-dependent H3K9me2 recruitment at the *G9a* promoter within the LA.

GluN2B mediates H/KMT-G9a and H/KDM-LSDI activity

Because H3K9me2 levels are determined by the opposing activities of enzymes H/KMT-G9a and H/KDM-LSD1, we next sought to determine whether the GluN2B subunit of the NMDA receptor regulated the recruitment of H/KMT-G9a and H/KDM-LSD1 at the *G9a* promoter within the LA. ChIP studies were performed following incubation of LA brain slices for 1 h with vehicle control alone (controls), NMDA alone (NMDA), NMDA plus Ro25-6981 (NMDA+Ro25-6981), or Ro25-6981 alone (Ro25-6981) (Fig. 7A). In concordance with our MK801 studies (Fig. 4), we observed main effects for H/KMT-G9a binding levels at *G9a* PW sites 1 ($H_{(4)} = 11.08$, $P < 0.01$), 2 ($H_{(4)} = 13.67$, $P < 0.01$), 4 ($H_{(4)} =$

A

B
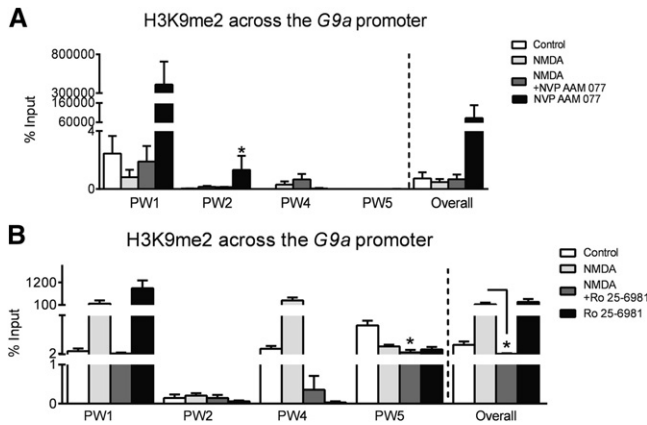
Figure 6. The GluN2B subunit of the NMDA receptor, but not the GluN2A subunit, regulates H3K9me2 levels at the *G9a* promoter. (*A*) LA slices were incubated with NMDA, NMDA+NVP AAM077, or NVP AAM077 alone for 1 h prior to ChIP analysis. There were increases in H3K9me binding at the *G9a* promoter observed in the NVP AAM 077 at PW site 2 relative to controls ($n = 3–5$). The overall profile of H3K9me2 binding at the *G9a* promoter upon NMDAR stimulation was not significantly altered by GluN2A subunit inhibition ($n = 12–15$). (*B*) LA slices were incubated with NMDA, NMDA+RO25-6981, or RO25-6981 alone for 1 h prior to ChIP analysis. There were increases in H3K9me binding at the *G9a* promoter observed in the NMDA group that were reversed in the NMDA+RO25-6981 group ($n = 3–5$). The overall profile of H3K9me2 binding at the *G9a* promoter revealed an increase in the presence of NMDA compared to the NMDA+RO25-6981 group ($n = 12–15$). (*) $P < 0.05$.

18.03, $P < 0.001$), and 5 ($H_{(4)} = 14.64$, $P < 0.01$). Importantly, increases in H/KMT-G9a binding levels at the *G9a* promoter at sites 2 and 5 in the NMDA group were significantly decreased in the NMDA+Ro25-6981 group. Interestingly, we found a significant increase in H/KMT-G9a binding at *G9a* PW site 1 in the Ro25-6981 group alone in comparison to controls, suggesting that GluN2B subunit inhibition alone in the absence of NMDAR activity can alter H/KMT-G9a recruitment at the *G9a* promoter. Additionally, we found a main effect for the overall profile of H/KMT-G9a binding across the *G9a* promoter ($H_{(4)} = 23.10$, $P < 0.001$). Dunn's post hoc tests revealed effects similar to the individual PW sites where H/KMT-G9a binding levels were increased at the *G9a* promoter in the NMDA group which was blocked by the addition of Ro25-6981. Together, these results further support the role of GluN2B subunit activity in the regulation of H/KMT-G9a recruitment at the gene promoters, such as *G9a* within the LA in response to NMDAR activation.

Intriguingly, H/KDM-LSD1 binding across the *G9a* promoter revealed differential results in the presence of GluN2B inhibitor Ro25-6981 in comparison to the nonselective NMDA receptor inhibitor MK801 (Fig. 7B). We found a main effect for H/KDM-LSD1 binding at *G9a* PW site 2 ($H_{(4)} = 8.059$, $P < 0.05$) but not sites 1 ($H_{(4)} = 5.365$, $P = 0.139$), 4 ($H_{(4)} = 0.333$, $P = 0.965$), or 5 ($H_{(4)} = 3.113$, $P = 0.402$). Surprisingly, inhibiting the GluN2B subunit in the presence of NMDA enhanced H/KDM-LSD1 binding at *G9a* PW site 2. These results allude to the possibility that the GluN2B subunit inhibits the recruitment of H/KDM-LSD1 at the *G9a* promoter. In the presence of NMDA, the antagonist Ro25-6981 inhibits GluN2B subunit, relieving the inhibition on H/KDM-LSD1, and resulting in enhanced H/KDM-LSD1 binding at *G9a* PW site 2. However, this would suggest that in the presence of NMDA alone we should have observed decreased H/KDM-LSD1 binding in comparison to the controls. It is important to note that the NMDAR agonist NMDA activates all NMDA receptors; howev-

er, we are blocking only GluN2B subunit containing subset of NMDARs. This may provide an explanation for the observed increases in H/KDM-LSD1 binding at *G9a* PW site 1 in the presence of NMDA agonist alone. These results suggest the possibility that potentially NMDARs lacking the GluN2B subunit regulate H/KDM-LSD1 recruitment at *G9a* PW sites 1, 4, and 5. Additionally, we found a main effect for G9a protein expression in the LA ($F_{(3,9)} = 13.53$, $P < 0.01$) (Fig. 7C) and Tukey post hoc tests revealed a decrease in H/KMT-G9a protein expression in the LA following NMDAR stimulation that was completely rescued by inhibiting GluN2B containing NMDARs. This decrease in H/KMT-G9a protein expression following NMDAR stimulation is consistent with the overall H3K9me2 ChIP analysis, which revealed a transcriptionally repressive chromatin microenvironment at the *G9a* promoter following NMDAR activation. Additionally, the rescue of these NMDAR-induced reductions in H/KMT-G9a protein expression by inhibition of GluN2B receptors is also consistent with our H3K9me2 ChIP analysis, which suggested that the NMDAR-induced transcriptionally repressive chromatin state was reversed with blockade of GluN2B subunits. Together, these results suggest that NMDAR-induced increases in H3K9me2 levels in the LA are regulated by GluN2B, but not GluN2A subunit containing NMDARs.

ERK is involved in H/KDM-LSD1 and H/KMT-G9a regulation by GluN2B

The extracellular signal-regulated kinase (ERK) is a downstream component of the NMDAR signal transduction pathway activated during memory formation (Schafe et al. 2000). Moreover, the GluN2B subunit of the NMDAR has been identified to be a crucial activator of ERK by enhancing phospho-ERK (pERK) levels

A

B

C
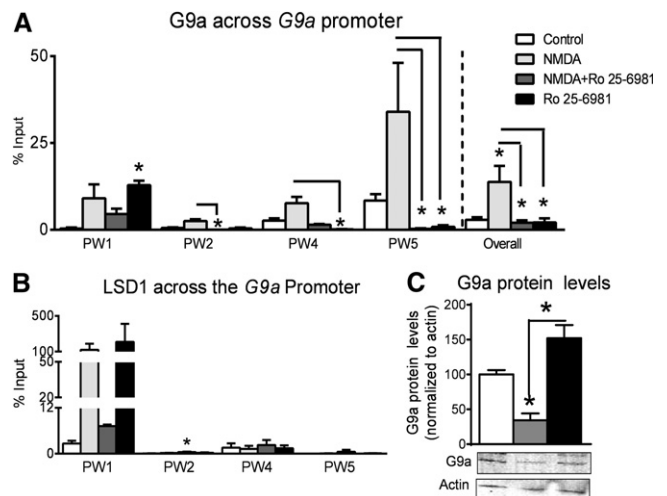
Figure 7. The GluN2B subunit of the NMDA receptor differentially regulates HMT-G9a, HDM-LSD1, and H3K9me2 recruitment at the *G9a* promoter in the LA. (*A*,*B*) LA slices were incubated with NMDA, NMDA+RO25-6981, or RO25-6981 alone for 1 h prior to ChIP analysis. (*A*) There were increases in HMT-G9a binding at the *G9a* promoter observed in the NMDA group that were reversed in the NMDA+RO25-6981 group ($n = 3–5$). The overall HMT-G9a occupancy at the *G9a* promoter revealed a significant increase in the presence of NMDA that was reduced in the NMDA+Ro25-6981 group ($n = 13–21$). (*B*) There were increased bindings of HDM-LSD1 to the *G9a* PW site 2 in the NMDA+RO25-6981 group relative to controls ($n = 3–5$). (*C*) Western blot analysis revealed significant decrease in G9a protein in NMDA group compared to controls that was reversed in the NMDA+RO25-6981 group ($n = 3–4$). (*) $P < 0.05$.
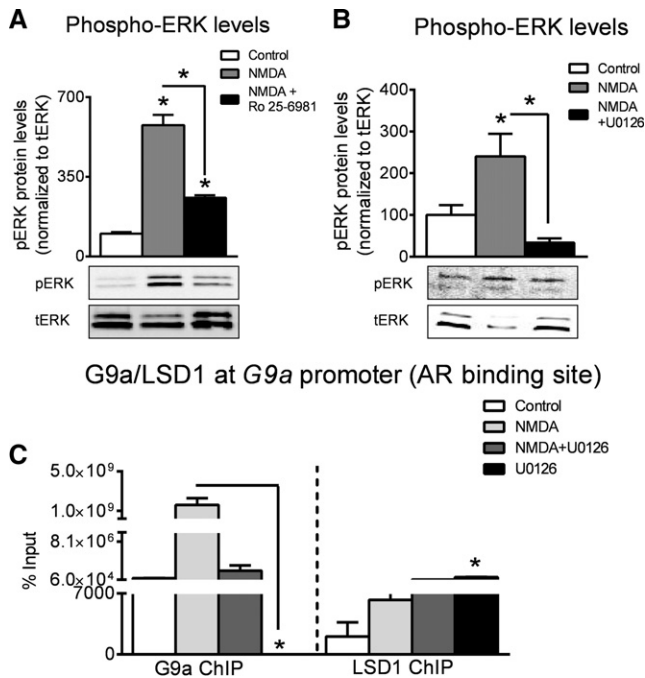
Figure 8. ERK activation drives GluN2B subunit-mediated regulation of H/KMT-G9a and H/KDM-LSD1 at the *G9a* promoter. (*A*) LA slices were incubated with NMDA or NMDA+RO25-6981 for 1 h. Western blot analysis revealed a significant increase in phospho-ERK protein levels in the NMDA group that was reversed in the NMDA+Ro25-6981 group (*n* = 3–4). (*B*) LA slices were incubated with NMDA or NMDA+U0126 for 1 h. Western blot analysis revealed a significant increase of phospho-ERK protein levels in the NMDA group that was reversed in the NMDA+U0126 group (*n* = 3–4). (*C*) LA slices were incubated with NMDA, NMDA+U0126, or U0126 for 1 h prior to ChIP analysis. There was an increase in HMT-G9a binding to the *G9a* promoter in the NMDA group relative to the U0126 group; however, U0126 enhanced HDM-LSD1 binding to the *G9a* promoter (*n* = 3–4). (*) *P* < 0.05.

(Krapivinsky et al. 2003) and GluN2B subunit activation enhances pERK levels in the LA during memory consolidation (Zhang et al. 2008). Thus, we determined the effect of GluN2B blockade on NMDAR-mediated ERK activation in the LA ex vivo. For these experiments, LA brain slices were isolated following incubation for 1 h with vehicle control alone (Control), NMDA alone (NMDA), NMDA plus Ro25-6981 (NMDA+Ro25-6981), or Ro25-6981 alone (Ro25-6981) (Fig. 8A). Western blotting analysis revealed a main effect for drug ($F_{(2,6)} = 25.74$, $P < 0.001$) and a significant increase in pERK levels in ex vivo LA brain slices with NMDA stimulation that were successfully blocked in the presence of the GluN2B antagonist Ro25-6981. As an additional control, we confirmed that NMDAR activation indeed coupled to ERK activation in LA brain slices following incubation for 1 h with vehicle control alone (Control), NMDA alone (NMDA), NMDA plus an inhibitor of ERK activation U0126 (NMDA+U0126), or U0126 alone (U0126) (Fig. 8B). We found a main effect for drug ($F_{(2,8)} =$

13.02, $P < 0.001$). Tukey post hoc tests revealed an increase in pERK levels in the NMDA group that were attenuated by the ERK inhibitor, confirming that we could successfully block ERK phosphorylation in the LA ex vivo with the MEK inhibitor U0126.

We next examined if ERK activation was necessary for NMDAR-induced binding of H/KMT-G9a and H/KMD-LSD1 to the *G9a* promoter in the amygdala. We restricted our ChIP analysis to *G9a* PW 1 as it contains the putative AR binding site present in the G9a promoter. We found a main effect for drug for H/KMT-G9a ($H_{(4)} = 8.667$, $P < 0.01$) binding activity at the *G9a* promoter (Fig. 8C). We found a significant decrease in the U0126 group compared to NMDA group and a reduction in the NMDA+U0126 group compared to the NMDA group, suggesting that ERK activity was necessary for the increased binding of H/KMT-G9a at the *G9a* promoter following NMDA stimulation. Additionally, we found a main effect for drug for H/KMD-LSD1 ($H_{(4)} = 10.08$, $P < 0.01$) binding activity at the *G9a* promoter (Fig. 8C). Interestingly, we found that the U0126 alone group showed significant decreases in H/KMT-G9a relative to the NMDA group and significant increases in H/KDM-LSD1 recruitment in comparison to controls. Collectively, these results support the hypothesis that the GluN2B subunit activates ERK which then drives the differential regulation of H/KMT-G9a and H/KDM-LSD1 at the *G9a* promoter, indicating that NMDAR-mediated H3K9me2 activity in the amygdala is largely regulated through ERK signaling.

H/KDM-LSD1 inhibition rescues the memory deficits

Thus far, our data suggest that GluN2B containing NMDARs regulate H/KMT-G9a, H/KDM-LSD1, and H3K9me2 via ERK activation in ex vivo LA brain slices. However, these studies do not functionally test our hypothesis at the behavioral level. Because we found that inhibition of H/KDM-LSD1 in the LA resulted in memory enhancement, we next extended our studies in-vivo to determine whether H/KDM-LSD1 inhibition could rescue the memory deficits caused by (1) inhibition of NMDAR signaling or (2) inhibition of ERK activation. For these experiments, animals received intraperitoneal (i.p.) injections of saline or MK801 1.5 h prior to fear conditioning followed by bilateral infusions of saline or t-PCP into the LA 1 h prior (0.5 h after first injection) to fear conditioning (Fig. 9A). This resulted in four groups: (1) saline–
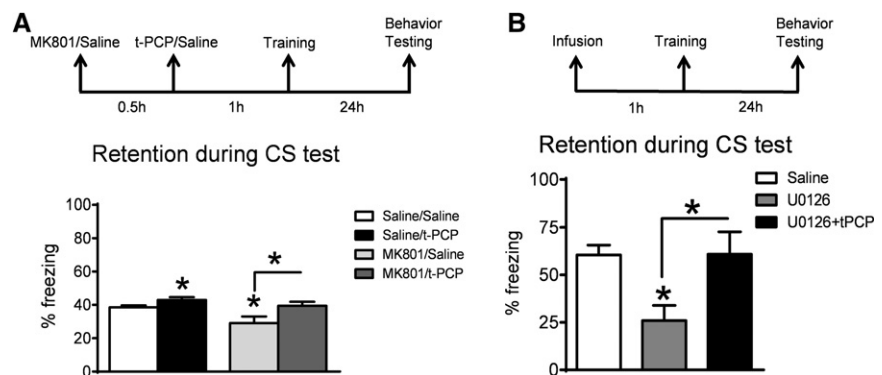
Figure 9. Inhibition of H/KDM-LSD1 in the LA rescued the memory deficits caused by NMDAR or ERK inhibition. (*A*) Animals were given an i.p. injection of saline or MK801 followed by an infusion of saline or t-PCP into the LA prior to fear conditioning. Saline/t-PCP infused animals froze significantly more than saline–saline controls on the long-term memory test while the MK801/saline infused animals froze significantly less than saline–saline controls. MK801/t-PCP infused animals froze significantly more than MK801/saline infused animals (*n* = 8–11). (*B*) Animals were infused with saline, U0126, or U0126+t-PCP into the LA prior to fear conditioning. U0126 infused animals froze significantly less than saline infused controls on the long-term memory test, while U0126+t-PCP infused animals froze significantly more than intra-LA U0126 infused animals (*n* = 6–8). (*) *P* < 0.05.

saline, (2) MK801–saline, (3) saline–t-PCP, and (4) MK801–t-PCP groups and all animals were tested for memory retention of the auditory cue 24 h later. We found a main effect for drug ($F_{(3,29)} = 6.734$, $P < 0.01$). As expected, we found a significant increase in the freezing behavior from saline–t-PCP animals compared to the saline–saline controls ($t_{(13)} = 2.161$, $P < 0.05$) and a significant decrease in freezing behavior from MK801–saline animals compared to the saline–saline controls ($t_{(15)} = 2.345$, $P < 0.05$). Intriguingly, we found a significant enhancement in the freezing behavior of MK801–t-PCP animals compared to MK801–saline animals ($t_{(15)} = 2.425$, $P < 0.05$) suggesting that H/KDM-LSD1 inhibition successfully rescued the memory deficits caused by NMDAR blockade within the LA.

Next, we examined if inhibition of H/KDM-LSD1 could rescue memory impairments caused by inhibiting ERK activation (Fig. 9B). Animals were divided into three groups that received pretraining infusions of (1) saline, (2) U0126, or (3) U0126+t-PCP into the LA 1 h prior to fear conditioning. All animals were tested for memory for the auditory cue 24 h later after behavioral training. We found a main effect for drug ($F_{(2,18)} = 6.051$, $P < 0.001$). In concurrence with previous findings (Schafe et al. 2000), we found a significant decrease in the freezing behavior of U0126 animals compared to saline ($t_{(13)} = 3.719$, $P < 0.01$). Interestingly, we found a significant enhancement in the freezing behavior of U0126–t-PCP animals compared to U0126 animals ($t_{(11)} = 2.512$, $P < 0.05$). These results suggest that H/KDM-LSD1 inhibition successfully rescued the memory deficits caused by inhibition of ERK activation within the LA. Collectively, these results suggest that GluN2B containing NMDAR activity increases ERK phosphorylation in the LA following fear conditioning, which is necessary for increases in H3K9me2 that results in the repression of gene transcription that is critical for fear memory consolidation.

Discussion

Epigenetic mechanisms have been widely implicated in transcriptional regulation of genes in several brain regions during the memory consolidation process (Levenson et al. 2004, 2006; Monsey et al. 2011). More recently, histone methylation has been shown to be critically involved during memory consolidation in both the entorhinal cortex and the hippocampus (Gupta et al. 2010; Gupta-Agarwal et al. 2012; Mahan et al. 2012). However, relatively little is known about the role of histone methylation in LA-dependent learning and memory. Furthermore, the regulation of H/KMTs and H/KDMs during memory consolidation has not been previously elucidated. In the present study, we found that regulation of the transcription repressive mark H3K9me2 was critical for fear memory formation in the LA. Pharmacological studies in conjunction with behavioral evidence revealed that while inhibiting increases in H3K9me2 levels in the LA caused memory deficits, increasing H3K9me2 levels in the LA resulted in memory enhancements. Additionally, we found that fear conditioning led to decreases in *G9a* gene expression, which were regulated by NMDAR-mediated H/KMT-G9a, H3K9me2, and H/KDM-LSD1 binding at the *G9a* promoter in the LA. We also found that the GluN2B, but not the GluN2A, containing NMDARs was critical for the recruitment of H/KMT-G9a and H3K9me2 at the *G9a* promoter, and may serve to inhibit the recruitment of H/KDM-LSD1 at the *G9a* promoter. Interestingly, our studies suggest that GluN2B containing NMDARs mediate the recruitment of epigenetic enzymes H/KMT-G9a and H/KDM-LSD1 via ERK activation, which is known to be critical for memory consolidation in the LA, and that enhancing H3K9me2 levels through blockade of H/KDM-LSD1 activity rescues memory deficits produced by ERK signaling inhibition. Collectively, these results suggest that GluN2B containing NMDARs mediate learning-induced changes

in H3K9me2 levels in the LA via ERK activation. To our knowledge, this is the first evidence of NMDAR-mediated ERK-signaling regulation of histone methylation levels in the LA during memory formation.

Histone modifications serve to modulate the interaction between DNA and histones, directly affecting gene transcription. Histone methylation of varying degrees and at different amino acid targets can serve to recruit either corepressors or coactivators of transcription, thus making it a powerful regulator of gene transcription (Lachner and Jenuwein 2002; Lachner et al. 2003; Zhang et al. 2012). Previously, H3K9me2-mediated molecular connectivity had been suggested between the hippocampus and the entorhinal cortex during memory consolidation (Gupta-Agarwal et al. 2012). In these same studies, fear conditioning elicited an increase in H3K9me2 levels within the LA whereas tone/context presentations resulted in enhanced H3K4me3 levels (Gupta-Agarwal et al. 2012). Therefore, the H3K4me3 mark was regulated in response to auditory and spatial inputs alone within the LA, whereas the association of the tone with footshock altered H3K9me2 mark specifically within the LA. These findings indicate that the transcription repressive mark H3K9me2 was specific to associative fear learning within the LA.

As an extension of these prior studies, here we found that H3K9me2 methylation continued to be regulated in the LA 24 h after fear conditioning, a time point at which memories are thought to be in a maintenance phase (Kwapis et al. 2009). This suggests that changes in H3K9me2 might serve as a persistent transcriptional code for fear memory storage. Interestingly, the change in H3K9me2 at 24 h was opposite of what was observed in the LA at 1 h during the memory consolidation phase (Gupta-Agarwal et al. 2012). These results indicate that H3K9me2 methylation might differentially regulate gene transcription targets during memory consolidation compared to the maintenance phase of memory storage. Future studies will focus on directly examining whether H3K9me2 in the LA is a critical regulator of memory maintenance.

Using a combined pharmacological and behavioral approach, we further defined the importance of H3K9me2 regulation in the LA during memory consolidation. H3K9me2 levels are regulated by the epigenetic writer protein, H/KMT-G9a, and the antagonistic epigenetic eraser protein, H/KDM-LSD1 (Tachibana et al. 2001, 2002, 2005, 2008; Metzger et al. 2005). Therefore, we simulated a loss of function of H3K9me2 through infusions of UNC0224 in the LA, and found that G9a is a positive regulator of memory formation in the LA. Alternatively, intra-LA infusions of the H/KDM-LSD1 inhibitor t-PCP simulated gain of function of H3K9me2, resulting in memory enhancement. These results suggest that a balance between the activity of the H/KMT-G9a and the H/KDM-LSD1 dictate H3K9me2 levels within the LA during memory formation.

NMDARs have been established as coincident detectors within the LA during memory consolidation (Bauer et al. 2002; Silva 2003; Sah et al. 2008). Hypofunctioning NMDARs within the LA result in memory deficits and have been associated with cognitive deficits found comorbid with several neurological disorders (Schauz and Koch 2000). Indeed, inhibition of NMDA receptors elicits schizophrenic-like symptoms in humans and impairs LTP in the LA (Pollard et al. 2012). However, the molecular mechanisms still remain uncertain. Here our findings provide insights into the potential role of histone methylation mechanisms in NMDAR mediated memory deficits. Our results indicate that NMDAR activity plays a crucial role in regulating H/KMT-G9a, H/KDM-LSD1, and subsequent H3K9me2 at the *G9a* promoter within the LA during memory consolidation, suggesting that NMDAR activity regulates histone methylation mediated epigenetic changes in the LA during fear memory formation.

Additionally, in the current study we established that H/KDM-LSD1 is a downstream effector of NMDAR activity and inhibition of H/KDM-LSD1 enhances memory formation. This suggests that while NMDAR activity is critical for fear memory formation, it may also act as a constraint on memory strength. Interestingly, we successfully rescued memory deficits caused by NMDAR blockade by inhibiting H/KDM-LSD1 activity in the LA. Thus, these findings warrant further investigation into the use of H/KDM-LSD1 as a potential therapeutic target for treatment of neurological disorders associated with memory deficits.

Importantly, researchers have established that individual NMDAR subunits play a key role in NMDAR electrophysiological properties and involvement in memory formation (Monyer et al. 1994; Bauer et al. 2002; Furukawa et al. 2005). NMDARs present in the LA are largely composed of the GluN1 subunit coupled to either the GluN2A or GluN2B subunit (Foster et al. 2010). Findings have revealed that the GluN2B subunit in the LA is crucial for fear memory formation whereas the GluN2A subunit is more generally involved in synaptic transmission (Rodrigues et al. 2001). Indeed, blockade of GluN2B subunit results in memory deficits for auditory fear conditioning (Walker and Davis 2008; Zhang et al. 2008). In relation to histone methylation-mediated epigenetic regulation, we showed for the first time that GluN2B, but not the GluN2A, subunit of the NMDAR regulated H/KMT-G9a and H3K9me2 recruitment at the *G9a* promoter in the LA. Furthermore, we found that inhibition of the GluN2B subunit relieved the inhibition on H/KDM-LSD1. Together, these results indicate that the GluN2B subunit activation may serve to promote H3K9me2 levels by either promoting the recruitment of H/KMT-G9a to the gene promoter or by preventing the recruitment of H/KDM-LSD1at the *G9a* promoter. In addition, alterations observed in H3K9me2 binding levels at the *G9a* promoter in the absence of NMDAR activity and in the presence of GluN2A or GluN2B antagonist alone can be interpreted in two ways. First, inhibitor binding to the NMDAR subunit may result in a conformational change that is translated downstream to effect histone methylation in the LA. Second, under basal conditions marked by the lack of NMDAR activity, a specific histone methylation profile is maintained at the *G9a* promoter that is subsequently altered in response to NMDAR stimulation. Moreover, we report here that GluN2B subunit containing NMDARs mediate effects on H/KMT-G9a and H/KDM-LSD1 binding via ERK activation. Indeed, inhibition of ERK activation mirrors the downstream epigenetic effects observed with GluN2B subunit inhibition. More importantly, pharmacological inhibition of H/KDM-LSD1 successfully rescued the memory deficits caused by inhibition of ERK activation within the LA. Collectively, these results suggest that GluN2B containing NMDARs regulate H3K9me2 levels through ERK activation in the LA during memory formation.

In summary, our findings describe a set of studies to demonstrate NMDA mediated H3K9me2 activity within the LA and that this process is crucial for fear memory formation. Moreover, our findings provide the first evidence delineating the sequence of NMDAR-mediated signaling events regulating histone methylation changes within the LA during memory consolidation. Specifically, the GluN2B subunit of the NMDAR drives regulation of antagonistic enzymes H/KMT-G9a and H/KDM-LSD1 via ERK activation to regulate H3K9me2 levels at a specific candidate gene promoter within the LA. Finally, the findings presented here provide a possible new drug locus for treating cognitive deficits associated with a hypofunctioning NMDAR. This will have broad implications for the treatment of neurological disorders such as schizophrenia, depression, bipolar disorder, anxiety, and autism (Beneyto and Meador-Woodruff 2008; Anderson and Maes 2013; Gandal et al. 2012; Gonzalez-Burgos and Lewis 2012; Hamm et al. 2012).

Materials and Methods

Animals
Adult male Sprague-Dawley rats (250–300 g) were used for all experiments. Animals were housed under 12-h light–dark conditions and allowed access to rodent chow and water ad libitum. Animals were acclimatized to laboratory conditions and were handled at least 3 d prior to use. All procedures were performed with the approval of the University of Alabama Birmingham Institutional Animal Care and Use Committee and according to national guidelines and policies.

Auditory fear conditioning protocol
Animals were transported to the behavior room 30 min to 2 h prior to fear conditioning on experiment day. The animals were placed in chamber A and allowed to explore for 50 sec, followed by a 90-dB, 500-Hz tone for 20 sec co-terminating with a 2-sec, 0.5-mA footshock. The 2-sec/0.5-mA cue–shock pairing was repeated three times over a 6-min duration. Twenty-four hours later, animals were placed in a novel chamber B and freezing behavior was measured using the Noldus software in response to the 90-dB, 500-Hz tone in the absence of a footshock. The training for the tone-only procedure was identical except that the shock presentations were omitted. For the immediate shock control experiment, animals were placed into novel chamber A and immediately received three shock (2-sec/0.5-mA) presentations separated by 1 sec. The animals were then immediately removed from the chamber and returned to their homecages.

Cannulae implantation
Animals were bilaterally placed with a 31-gauge single-guide cannula, from which the injector projected 1 mm to end in intra-LA. The stereotaxic coordinates used for intra LA surgeries were AP, -3.2 mm from bregma; ML, ± 5.0 mm; DV, -8.0 mm from skull (Paxinos et al. 1980). Cresyl violet staining was performed to confirm cannula placement. Animals were habituated to dummy cannula removal and allowed to recover for 5 d prior to infusion and behavioral studies.

Drug
Animals were infused with either saline (0.9% NaCl, pH 7.4) or UNC0224 (conc. 15 nM, Cayman Chemical) or *trans*-2-phenylcyclopropylamine hydrochloride (conc. 2 μM, Sigma Chemical) 1 h prior to fear conditioning. Animals were i.p. injected with MK801 (conc. 300 μg/kg, Sigma Chemical) 1.5 h prior to fear conditioning. All drugs were diluted in saline.

Isolation of lateral amygdala (LA)
Whole brain was removed and placed in oxygenated (95%/5% O_2/CO_2), ice-cold cutting solution (composed of [in mM] 110 sucrose, 60 NaCl, 3 KCl, 1.25 NaH_2PO_4, 28 $NaHCO_3$, 0.5 $CaCl_2$, 7 $MgCl_2$, 5 glucose, and 0.6 ascorbate). The LA was microdissected using the rat brain matrix and flash frozen on dry ice. For the immediate shock control experiments, brains were rapidly removed, flash frozen on dry ice, and the LA microdissected using the rat brain matrix. All isolated tissue was stored at $-80°C$ for future processing.

Ex vivo pharmacological studies
One millimeter brain sections containing the LA were incubated for 40 min in 1:1 artificial cerebral spinal fluid (ACSF) (composed of [in g] 7.031 NaCl, 0.186 KCl, 0.203 $MgCl_2$, 0172 NaH_2PO_4, 2.1 $NaHCO_3$, and 4.51 glucose, and 900 mL water and 2 mL 1 M $CaCl_2$ at room temperature). Slices were removed and further incubated in 100% ACSF for 45 min at room temperature, then 100% ACSF for 1 h at 32°C. Drugs or vehicle were then added to the slices for 1 h before LA was dissected. All solutions were continuously bubbled with 95% O_2/5% CO_2. Drugs used: NMDA (100 mM, dissolved in saline, Sigma Chemicals), Ro 25-6981 (1 μM, dissolved

in saline, Sigma Chemicals), MK801 (60 nM, dissolved in saline), U0126 (20 μM, dissolved in DMSO, Promega), or NVP AAM 077 (0.1 μM, dissolved in saline, Sigma Chemicals). All isolated tissue was stored at −80°C for future processing.

Histone extraction

Histone extraction was performed as previously described in Lubin et al. (2008), Gupta et al. (2010), and Gupta-Agarwal et al. (2012). Briefly, homogenized tissue was subjected to centrifugation at 7700g for 1 min. The nuclei containing pellet was resuspended in 250 μL of 0.4 N H_2SO_4, incubated on ice for 30 min, and then centrifuged at 4°C for 30 min at 14,000g. Precipitated protein was recovered by centrifugation and followed by acetone drying. All procedures were carried out under ice-cold conditions. The purified histone enriched protein pellet was resuspended in 10 mM Tris (pH 8.0). Protein concentrations were determined via the Bio-Rad protein assay reagent.

Western blotting

For quantification of histone methylation levels, histone protein extracts (1–10 μg) were separated on a 12% or 20% polyacrylamide gel with a 4% stacking gel. The histone proteins were transferred onto an Immobilon-FL membrane which was then probed with primary antibodies for H3K9me2 (1:500; Millipore, #07-441), H3K4me3 (1:500; Millipore, #04-745), TH3 (1:1000; Abcam, #ab10799), G9a (1:1000; Abcam, #ab40542), pERK1/2 (1:1000; Cell Signal, #4370), tERK1/2 (1:1000; Upstate, #06182), and β-actin (1:1000; Abcam, #ab8229). Secondary goat anti-rabbit 700CW or 800CW antibody (1:20,000; Licor Biosciences) was used for detection of histone protein using the Licor Odyssey system. All quantifications were normalized to respective total proteins (TH3 or tERK1/2) levels or β-actin levels.

Nuclear extraction

Nuclear and cytoplasmic extracts were prepared using Thermo scientific NE-PER nuclear and cytoplasmic extraction reagents (#78833) and stored at −80°C for future processing.

Measuring mRNA levels by real-time, reverse transcription PCR

Isolated LA tissue was subjected to RNA extraction using the All Prep DNA/RNA mini kit (Qiagen, #80204). RNA was converted to cDNA using the iScript cDNA synthesis kit (Bio-Rad). All cDNA samples were preamplified at 95°C for 10 min, 20 repeats of 95°C for 15 sec and 60°C for 1 min, and finally hold at 4°C. RT-PCR amplifications were performed on the iQ5 real-time PCR system (Bio-Rad) at 95°C for 3 min, 50 repeats of 95°C for 10 sec followed by 62°C for 30 sec, 95°C for 1 min, 55°C for 1 min, 81 repeats of 55°C for 10 sec each, and finally hold at 4°C, using primer sets specific to regions of interest in the *cFOS* (forward: CCCGTAGACCTAGGGAGGAC, reverse: CAATACACTCCATGCGGTTG), *Zif268* (forward: TCAGCCTAGTCAGTGGCCTT, reverse: AGGTCTCCCTGTTGTTGTGG), *BDNF exon IV* (forward: TGCGAGTATTACCTCCGCCAT, reverse: TCACGTGCTCAAAAGTGTCAG), *G9a* (forward: CCCAGAGGAGTGAATGGTGT, reverse: CTTTCGGTGGCCATACACTT) gene promoters. Quantification of β−tubulin-4 levels (forward: AGCAACATGAATGACCTGGTG, reverse: GCTTTCCCTAACCTGCTTGG) was used as internal control for normalization.

Chromatin immunoprecipitation (ChIP)

ChIP assays were performed as previously described in Lubin et al. (2008). Chromatin was sheared using a Branson Sonifier 250 at 1.5 power and constant duty cycle. Lysates were centrifuged to pellet debris and then diluted 1:10 in ChIP dilution buffer (16.7 mM Tris, pH 8.1, 0.01% SDS, 1.1% Triton X-100, 167 mM NaCl, 1.2 mM EDTA). Extracts were precleared for 45 min with a 50% suspension of salmon sperm-saturated protein A. Immunoprecipitations were carried out at 4°C overnight with primary antibodies

(anti-acetyl H3, -acetyl H4, -phosphoacetyl H3) or No antibody (control). Immune complexes were collected with protein A and sequentially washed with low salt buffer (20 mM Tris, pH 8.0, 0.1% SDS, 1% Triton X-100, 2 mM EDTA, 150 mM NaCl), high salt buffer (20 mM Tris, pH 8.1, 0.1% SDS, 1% Triton X-100, 500 mM NaCl, 1 mM EDTA), LiCl immune complex buffer (0.25 M LiCl, 10 mM Tris, pH 8.1, 1% deoxycholic acid, 1% IGEPAL-CA630, 500 mM NaCl, 2 mM EDTA), and TE buffer. Immune complexes were extracted in 1× TE containing 1% SDS, and protein-DNA cross-links were reverted by heating at 65°C overnight. After proteinase K digestion (100 μg, 2 h at 37°C), DNA was extracted by phenol/chloroform/isoamyl alcohol and then ethanol precipitated. Immunoprecipitated DNA was preamplified using the thermocycler at 95°C for 10 min, 20 repeats of 95°C for 15 sec and 60°C for 1 min, and hold at 4°C. All DNA samples were subjected to quantitative real-time PCR using primers specific to the rat *G9a PW* sites. *G9a PW 1* (forward: CGGCTCAGAACCAGAAAGAC, reverse: TCCAGAACTGGGGTTGTAGG) *G9a PW 2* (forward: TCCTTTAAGGCGTCTTCTCG, reverse: CTCTCCCCCTCCCCTTCC) *G9a PW 3* (forward: GCTTTATGCTTGTGGGTGGT, reverse: CAGCAATGAGAGCAGTTGGA) *G9a PW 4* (forward: TTGGTGGCACACGACTTTAG, reverse: CCGCAAACATGTCCTCTTCT) *G9a PW 5* (forward: TGAATGTCAACATCGGCAGT, reverse: TGGGGAATTTAGCTCAGTGG) *G9a PW 6* (forward: GTCCCCAGGCACATCTTTTA, reverse: AAACCCACAGGTCTCTGACG) *G9a PW 7* (forward: CAGACACAACACTCGCACCT, reverse: CCCTGTCTCGAGAACACACA). The cumulative fluorescence for each amplicon was normalized to input amplification.

Transcription factor analysis

Briefly, upstream promoter sequence information for the *G9a* was obtained using the DBTSS website http://dbtss.hgc.jp/. To identify putative transcription factor binding sites, 5000 bp of the upstream sequence were examined using the transcription factor search, http://www.cbrc.jp/research/db/TFSEARCH.html, and the JASPAR database, http://jaspar.genereg.net/cgi-bin/jaspar_db.pl?rm=browse&db=core&tax_group=vertebrates.

Statistical analysis

Comparison between groups for western blotting results was done using one-way ANOVA with Tukey's post hoc test or Student's *t*-test. All ChIP analyses were done using the nonparametric Kruskal–Wallis ANOVA and Dunn's post hoc test. Behavioral characterization of the saline versus drug infused animal was done using Student *t*-test.

Acknowledgments

References

Akbarian S, Huang HS. 2009. Epigenetic regulation in human brain—focus on histone lysine methylation. *Biol Psychiatry* **65:** 198–203.

Anderson G, Maes M. 2013. Schizophrenia: linking prenatal infection to cytokines, the tryptophan catabolite (TRYCAT) pathway, NMDA receptor hypofunction, neurodevelopment and neuroprogression. *Prog Neuropsychopharmacol Biol Psychiatry* **42:** 5–19.

Bailey DJ, Kim JJ, Sun W, Thompson RF, Helmstetter FJ. 1999. Acquisition of fear conditioning in rats requires the synthesis of mRNA in the amygdala. *Behav Neurosci* **113:** 276–282.

Bauer EP, Schafe GE, LeDoux JE. 2002. NMDA receptors and L-type voltage-gated calcium channels contribute to long-term potentiation and different components of fear memory formation in the lateral amygdala. *J Neurosci* **22:** 5239–5249.

Benelkebir H, Hodgkinson C, Duriez PJ, Hayden AL, Bulleid RA, Crabb SJ, Packham G, Ganesan A. 2011. Enantioselective synthesis of tranylcypromine analogues as lysine demethylase (LSD1) inhibitors. *Bioorg Med Chem* **19:** 3709–3716.

Beneyto M, Meador-Woodruff JH. 2008. Lamina-specific abnormalities of NMDA receptor-associated postsynaptic protein transcripts in the prefrontal cortex in schizophrenia and bipolar disorder. *Neuropsychopharmacology* **33:** 2175–2186.

Binda C, Valente S, Romanenghi M, Pilotto S, Cirilli R, Karytinos A, Ciossani G, Botrugno OA, Forneris F, Tardugno M, et al. 2010. Biochemical, structural, and biological evaluation of tranylcypromine derivatives as inhibitors of histone demethylases LSD1 and LSD2. *J Am Chem Soc* **132:** 6827–6833.

Chwang WB, O'Riordan KJ, Levenson JM, Sweatt JD. 2006. ERK/MAPK regulates hippocampal histone phosphorylation following contextual fear conditioning. *Learn Mem* **13:** 322–328.

Covington HE III, Maze I, Sun H, Bomze HM, DeMaio KD, Wu EY, Dietz DM, Lobo MK, Ghose S, Mouzon E, et al. 2011. A role for repressive histone methylation in cocaine-induced vulnerability to stress. *Neuron* **71:** 656–670.

Fischer G, Mutel V, Trube G, Malherbe P, Kew JN, Mohacsi E, Heitz MP, Kemp JA. 1997. Ro 25-6981, a highly potent and selective blocker of N-methyl-D-aspartate receptors containing the NR2B subunit. Characterization in vitro. *J Pharmacol Exp Ther* **283:** 1285–1292.

Flores-Soto ME, Chaparro-Huerta V, Escoto-Delgadillo M, Vazquez-Valls E, Gonzalez-Castaneda RE, Beas-Zarate C. 2012. Structure and function of NMDA-type glutamate receptor subunits. *Neurologia* **27:** 301–310.

Foster KA, McLaughlin N, Edbauer D, Phillips M, Bolton A, Constantine-Paton M, Sheng M. 2010. Distinct roles of NR2A and NR2B cytoplasmic tails in long-term potentiation. *J Neurosci* **30:** 2676–2685.

Furukawa H, Singh SK, Mancusso R, Gouaux E. 2005. Subunit arrangement and function in NMDA receptors. *Nature* **438:** 185–192.

Gandal MJ, Anderson RL, Billingslea EN, Carlson GC, Roberts TP, Siegel SJ. 2012. Mice with reduced NMDA receptor expression: more consistent with autism than schizophrenia? *Genes Brain Behav* **11:** 740–750.

Gonzalez-Burgos G, Lewis DA. 2012. NMDA receptor hypofunction, parvalbumin-positive neurons, and cortical γ oscillations in schizophrenia. *Schizophr Bull* **38:** 950–957.

Gupta S, Kim SY, Artis S, Molfese DL, Schumacher A, Sweatt JD, Paylor RE, Lubin FD. 2010. Histone methylation regulates memory formation. *J Neurosci* **30:** 3589–3599.

Gupta-Agarwal S, Franklin AV, Deramus T, Wheelock M, Davis RL, McMahon LL, Lubin FD. 2012. G9a/GLP histone lysine dimethyltransferase complex activity in the hippocampus and the entorhinal cortex is required for gene activation and silencing during memory consolidation. *J Neurosci* **32:** 5440–5453.

Hamm JP, Gilmore CS, Clementz BA. 2012. Augmented γ band auditory steady-state responses: support for NMDA hypofunction in schizophrenia. *Schizophr Res* **138:** 1–7.

Jarome TJ, Helmstetter FJ. 2013. The ubiquitin–proteasome system as a critical regulator of synaptic plasticity and long-term memory formation. *Neurobiol Learn Mem* **105:** 107–116.

Jarome TJ, Lubin FD. 2013. Histone lysine methylation: critical regulator of memory and behavior. *Rev Neurosci* **24:** 375–387.

Jarome TJ, Werner CT, Kwapis JL, Helmstetter FJ. 2011. Activity dependent protein degradation is critical for the formation and stability of fear memory in the amygdala. *PLoS One* **6:** e24349.

Johansen JP, Cain CK, Ostroff LE, LeDoux JE. 2011. Molecular mechanisms of fear learning and memory. *Cell* **147:** 509–524.

Koshibu K, Graff J, Beullens M, Heitz FD, Berchtold D, Russig H, Farinelli M, Bollen M, Mansuy IM. 2009. Protein phosphatase 1 regulates the histone code for long-term memory. *J Neurosci* **29:** 13079–13089.

Krapivinsky G, Krapivinsky L, Manasian Y, Ivanov A, Tyzio R, Pellegrino C, Ben-Ari Y, Clapham DE, Medina I. 2003. The NMDA receptor is coupled to the ERK pathway by a direct interaction between NR2B and RasGRF1. *Neuron* **40:** 775–784.

Kwapis JL, Jarome TJ, Lonergan ME, Helmstetter FJ. 2009. Protein kinase Mζ maintains fear memory in the amygdala but not in the hippocampus. *Behav Neurosci* **123:** 844–850.

Lachner M, Jenuwein T. 2002. The many faces of histone lysine methylation. *Curr Opin Cell Biol* **14:** 286–298.

Lachner M, O'Sullivan RJ, Jenuwein T. 2003. An epigenetic road map for histone lysine methylation. *J Cell Sci* **116:** 2117–2124.

LeDoux JE. 2000. Emotion circuits in the brain. *Annu Rev Neurosci* **23:** 155–184.

Levenson JM, O'Riordan KJ, Brown KD, Trinh MA, Molfese DL, Sweatt JD. 2004. Regulation of histone acetylation during memory formation in the hippocampus. *J Biol Chem* **279:** 40545–40559.

Levenson JM, Roth TL, Lubin FD, Miller CA, Huang IC, Desai P, Malone LM, Sweatt JD. 2006. Evidence that DNA (cytosine-5) methyltransferase regulates synaptic plasticity in the hippocampus. *J Biol Chem* **281:** 15763–15773.

Liu F, Chen X, Allali-Hassani A, Quinn AM, Wasney GA, Dong A, Barsyte D, Kozieradzki I, Senisterra G, Chau I, et al. 2009. Discovery of a 2,4-diamino-7-aminoalkoxyquinazoline as a potent and selective inhibitor of histone lysine methyltransferase G9a. *J Med Chem* **52:** 7950–7953.

Lubin FD, Roth TL, Sweatt JD. 2008. Epigenetic regulation of BDNF gene transcription in the consolidation of fear memory. *J Neurosci* **28:** 10576–10586.

Lubin FD, Gupta S, Parrish RR, Grissom NM, Davis RL. 2011. Epigenetic mechanisms: critical contributors to long-term memory formation. *Neuroscientist* **17:** 616–632.

Mahan AL, Mou L, Shah N, Hu JH, Worley PF, Ressler KJ. 2012. Epigenetic modulation of Homer1a transcription regulation in amygdala and hippocampus with pavlovian fear conditioning. *J Neurosci* **32:** 4651–4659.

Malkani S, Rosen JB. 2001. N-Methyl-D-aspartate receptor antagonism blocks contextual fear conditioning and differentially regulates early growth response-1 messenger RNA expression in the amygdala: implications for a functional amygdaloid circuit of fear. *Neuroscience* **102:** 853–861.

Mallon AP, Auberson YP, Stone TW. 2005. Selective subunit antagonists suggest an inhibitory relationship between NR2B and NR2A-subunit containing N-methyl-D-aspartate receptors in hippocampal slices. *Exp Brain Res* **162:** 374–383.

Marek GJ, Behl B, Bespalov AY, Gross G, Lee Y, Schoemaker H. 2010. Glutamatergic (N-methyl-D-aspartate receptor) hypofrontality in schizophrenia: too little juice or a miswired brain? *Mol Pharmacol* **77:** 317–326.

Martin C, Zhang Y. 2005. The diverse functions of histone lysine methylation. *Nat Rev Mol Cell Biol* **6:** 838–849.

Metzger E, Wissmann M, Yin N, Muller JM, Schneider R, Peters AH, Gunther T, Buettner R, Schule R. 2005. LSD1 demethylates repressive histone marks to promote androgen-receptor-dependent transcription. *Nature* **437:** 436–439.

Monsey MS, Ota KT, Akingbade IF, Hong ES, Schafe GE. 2011. Epigenetic alterations are critical for fear memory consolidation and synaptic plasticity in the lateral amygdala. *PLoS One* **6:** e19958.

Monyer H, Burnashev N, Laurie DJ, Sakmann B, Seeburg PH. 1994. Developmental and regional expression in the rat brain and functional properties of four NMDA receptors. *Neuron* **12:** 529–540.

Parsons RG, Gafford GM, Helmstetter FJ. 2006. Translational control via the mammalian target of rapamycin pathway is critical for the formation and stability of long-term fear memory in amygdala neurons. *J Neurosci* **26:** 12977–12983.

Paxinos G, Watson CR, Emson PC. 1980. AChE-stained horizontal sections of the rat brain in stereotaxic coordinates. *J Neurosci Methods* **3:** 129–149.

Phillips RG, LeDoux JE. 1992. Differential contribution of amygdala and hippocampus to cued and contextual fear conditioning. *Behav Neurosci* **106:** 274–285.

Pollard M, Varin C, Hrupka B, Pemberton DJ, Steckler T, Shaban H. 2012. Synaptic transmission changes in fear memory circuits underlie key features of an animal model of schizophrenia. *Behav Brain Res* **227:** 184–193.

Rea S, Eisenhaber F, O'Carroll D, Strahl BD, Sun ZW, Schmid M, Opravil S, Mechtler K, Ponting CP, Allis CD, et al. 2000. Regulation of chromatin structure by site-specific histone H3 methyltransferases. *Nature* **406:** 593–599.

Rodrigues SM, Schafe GE, LeDoux JE. 2001. Intra-amygdala blockade of the NR2B subunit of the NMDA receptor disrupts the acquisition but not the expression of fear conditioning. *J Neurosci* **21:** 6889–6896.

Sah P, Westbrook RF, Luthi A. 2008. Fear conditioning and long-term potentiation in the amygdala: what really is the connection? *Ann N Y Acad Sci* **1129:** 88–95.

Schafe GE, Atkins CM, Swank MW, Bauer EP, Sweatt JD, LeDoux JE. 2000. Activation of ERK/MAP kinase in the amygdala is required for memory consolidation of pavlovian fear conditioning. *J Neurosci* **20:** 8177–8187.

Schauz C, Koch M. 2000. Blockade of NMDA receptors in the amygdala prevents latent inhibition of fear-conditioning. *Learn Mem* **7:** 393–399.

Schito AM, Pizzuti A, Di Maria E, Schenone A, Ratti A, Defferrari R, Bellone E, Mancardi GL, Ajmar F, Mandich P. 1997. mRNA distribution in adult human brain of GRIN2B, a N-methyl-D-aspartate (NMDA) receptor subunit. *Neurosci Lett* **239:** 49–53.

Schneider R, Bannister AJ, Myers FA, Thorne AW, Crane-Robinson C, Kouzarides T. 2004. Histone H3 lysine 4 methylation patterns in higher eukaryotic genes. *Nat Cell Biol* **6:** 73–77.

Silva AJ. 2003. Molecular and cellular cognitive studies of the role of synaptic plasticity in memory. *J Neurobiol* **54:** 224–237.

Son GH, Geum D, Chung S, Kim EJ, Jo JH, Kim CM, Lee KH, Kim H, Choi S, Kim HT, et al. 2006. Maternal stress produces learning deficits associated with impairment of NMDA receptor-mediated synaptic plasticity. *J Neurosci* **26:** 3309–3318.

Szakacs R, Janka Z, Kalman J. 2012. The "blue" side of glutamatergic neurotransmission: NMDA receptor antagonists as possible novel therapeutics for major depression. *Neuropsychopharmacol Hung* **14:** 29–40.

Tachibana M, Sugimoto K, Fukushima T, Shinkai Y. 2001. Set domain-containing protein, G9a, is a novel lysine-preferring mammalian histone methyltransferase with hyperactivity and specific selectivity to lysines 9 and 27 of histone H3. *J Biol Chem* **276:** 25309–25317.

Tachibana M, Sugimoto K, Nozaki M, Ueda J, Ohta T, Ohki M, Fukuda M, Takeda N, Niida H, Kato H, et al. 2002. G9a histone methyltransferase plays a dominant role in euchromatic histone H3 lysine 9 methylation and is essential for early embryogenesis. *Genes Dev* **16:** 1779–1791.

Tachibana M, Ueda J, Fukuda M, Takeda N, Ohta T, Iwanari H, Sakihama T, Kodama T, Hamakubo T, Shinkai Y. 2005. Histone methyltransferases G9a and GLP form heteromeric complexes and are both crucial for methylation of euchromatin at H3-K9. *Genes Dev* **19:** 815–826.

Tachibana M, Matsumura Y, Fukuda M, Kimura H, Shinkai Y. 2008. G9a/GLP complexes independently mediate H3K9 and DNA methylation to silence transcription. *EMBO J* **27:** 2681–2690.

Tang YP, Shimizu E, Dube GR, Rampon C, Kerchner GA, Zhuo M, Liu G, Tsien JZ. 1999. Genetic enhancement of learning and memory in mice. *Nature* **401:** 63–69.

Walker DL, Davis M. 2008. Amygdala infusions of an NR2B-selective or an NR2A-preferring NMDA receptor antagonist differentially influence fear conditioning and expression in the fear-potentiated startle test. *Learn Mem* **15:** 67–74.

Wang J, Scully K, Zhu X, Cai L, Zhang J, Prefontaine GG, Krones A, Ohgi KA, Zhu P, Garcia-Bassets I, et al. 2007. Opposing LSD1 complexes function in developmental gene activation and repression programmes. *Nature* **446:** 882–887.

Zhang XH, Liu F, Chen Q, Zhang CL, Zhuo M, Xiong ZQ, Li BM. 2008. Conditioning-strength dependent involvement of NMDA NR2B subtype receptor in the basolateral nucleus of amygdala in acquisition of auditory fear memory. *Neuropharmacology* **55:** 238–246.

Zhang X, Wen H, Shi X. 2012. Lysine methylation: beyond histones. *Acta Biochim Biophys Sin (Shanghai)* **44:** 14–27.